Electronic supplementary materials *Mendeleev Commun.*, 2024, **34**, 484–487

Synthesis, structure, and photoluminescent properties of a mixed carboxylate pentafluorobenzoate–phenylacetate complex of terbium

**Natalia V. Gogoleva, Maxim A. Shmelev, Aleksandr S. Chistyakov,
Galina A. Razgonyaeva, Vladislav M. Korshunov, Alisia V. Tsorieva, Ilya V. Taydakov,
Alexey A. Sidorov and Igor L. Eremenko**

Contents

I. Supplementary synthetic data

Synthesis of all obtained compounds was carried out in air using EtOH (96%), MeCN (99,9%), $Tb(OAc)_3 \cdot 5H_2O$ (Lanhit, 99,99%), 2,3,4,5,6-pentafluorobenzoic acid (H(pfb), 99%, “P&M-Invest”), phenylacetic acid (H(PhAc), 99%), 1,10-phenanthroline monohydrate (phen · H_2O, 99%, “Aldrich-Chemie”). $[Tb(H_2O)_4(pfb)_3]$ was synthesized using a known procedure[S1].

Infrared spectra of the complexes **1-3** were recorded in the frequency range 4000–400 cm^{-1} on a Perkin-Elmer Spectrum 65 Fourier transform infrared spectrometer equipped with Quest ATR Accessory (Specac). Elemental CHNS analysis of the synthesized compounds was carried out on a EuroEA 3000 CHNS analyzer (EuroVector, S.p.A.).

The powder diffraction patterns were obtained using the Bruker D8 Advance diffractometer with a LynxEye detector in Bragg-Brentano geometry. The sample was finely dispersed on a silicon holder with a zero background, $\lambda(CuK\alpha) = 1.54060$ Å. The acquired data were refined using the Topas 4 software[S2].

Photoluminescence excitation, emission spectra, and luminescence decays were recorded at room temperature with a Horiba-Jobin-Yvon Fluorolog-QM spectrofluorimeter equipped with a 75 W ArcTune xenon lamp and a Hamamatsu R-FL-QM-R13456 photomultiplier sensitive in the 200-980 nm emission range. The luminescence quantum yield (Φ) values were measured by absolute method, employing the same setup equipped with a G8 Spectralon®- covered sphere (GMP SA, Switzerland) and Hamamatsu R13456 photomultiplier. A diffusing screen was mounted inside the sphere to avoid direct irradiation of the detector. The measurements were carried out at ambient temperature. The samples in quartz cells were placed near the center of the sphere. A NIST-traceable 45 W quartz tungsten-halogen bulb emission standard (Oriel) was employed to measure the instrument response function. All QY measurements were repeated at least three times to achieve an experimental error below 15%.

Synthesis of $[Tb_2(phen)_2(pfb)_4(PhAc)_2]$ (1)

Method A.

To a solution of $Tb(OAc)_3 \cdot 5H_2O$ (0.075 g, 0.176 mmol) in 10 mL of MeCN and 5 mL of EtOH, a solution of H(PhAc) (0.048 g, 0.352 mmol) and H(pfb) (0.037 g, 0.176 mmol) in 10 mL of MeCN and 5 mL of EtOH was added. After stirring the reaction mixture for 5 minutes, phen·H_2O (0.035 g, 0.176 mmol) was added, leading to the formation of a white amorphous precipitate. The precipitate was filtered, and the mother liquor was left to evaporate slowly at room temperature. After 7 days, colorless crystals suitable for X-ray diffraction analysis had formed.

These crystals were washed with EtOH at room temperature and dried in open air. The yield of complex **1** was 0.058 g (36.8% based on the initial amount of $Tb(OAc)_3{\cdot}5H_2O$).

Method B.

To a solution of $Tb(OAc)_3{\cdot}5H_2O$ (0.050 g, 0.117 mmol) in 10 mL of MeCN, a solution of H(PhAc) (0.016 g, 0.117 mmol) and H(pfb) (0.050 g. 0.234 mmol) in 10 mL of EtOH was added. After stirring the reaction mixture for 5 minutes, $phen{\cdot}H_2O$ (0.023 g, 0.117 mmol) was added, leading to the formation of a white amorphous precipitate. The precipitate was filtered, and the mother liquor was left to evaporate slowly at room temperature. After 10 days, colorless crystals suitable for X-ray diffraction analysis formed. These crystals were washed with cold EtOH at room temperature and dried in open air. The yield of complex **1** was 0.048 g (45.8% based on the initial amount of $Tb(OAc)_3{\cdot}5H_2O$).

Found, %: C 45.6, H 1.9, N 3.2;

For $C_{68}H_{30}F_{20}N_4O_{12}Tb_2$

Calculated, %:C 45.5, H 1.7, N 3.1;

IR spectrum (ATR method; ν, cm^{-1}): 1635 s, 1580 m, 1518 m, 1486 m, 1422 s, 1395 s, 1344 w, 1296 w, 1143 w, 1106 m, 990 s, 942 w, 862 w, 848 m, 828 w, 762 s, 730 m, 722 m, 705 s, 637 w, 616 w, 566 w.

Synthesis of $[Tb_2(phen)_2(PhAc)_6]$ (2)

The terbium(III) acetate (0.100 g, 0.225 mmol) and phenylacetic acid (0.092 g, 0.675 mmol) were dissolved in 20 mL of EtOH with heating to 70°C and constant stirring. After the complete dissolution of the components, the reaction mixture was cooled to room temperature, and 1,10-phenanthroline (0.045 g, 0.225 mmol) was added. The formation of a white suspension was observed. Upon adding a mixture of 5 mL of acetonitrile and 5 mL of benzene, the suspension was completely dissolved. The reaction mixture was left to slowly evaporate at room temperature. After two days, colorless crystals suitable for X-ray diffraction analysis formed. The crystals of compound 2 were filtered and washed with cold MeCN. The yield of compound **2** was 0.119 g (68.6% based on $Tb(OAc)_3{\cdot}5H_2O$).

Found, %: C 57.9 H 3.7 N 3.7

For $C_{72}H_{58}N_4O_{12}Tb_2$

Calculated, %:C 58.1 H 3.9 N 3.8

IR spectrum (ATR method; ν, cm^{-1}): 3085 w, 3061 w, 3029 w, 2909 w, 1602 s, 1590 m, 1549 m, 1517 m, 1496 m, 1451 m, 1427 s, 1399 s, 1348 m, 1288 m, 1225 w, 1201 w, 1190 w, 1183 w, 1143 w, 1100 w, 1083 w, 1074 w, 1049 w, 1030 w, 1009 w, 996 w, 955 w, 932 w, 864 w, 846 m, 787 w, 769 w, 752 w, 730 m, 708 s, 671 m, 653 w, 637 m, 615 m, 585 w, 571 w, 558 w

Synthesis of [$Tb_2(EtOH)_2(phen)_2(pfb)_6$] (3)

Complex [$Tb(H_2O)_4(pfb)_3$] (0.050 g, 0.058 mmol) was dissolved in 10 mL of EtOH for one hour at a temperature of 60°C, after that 1,10-phenanthroline (0.011 g, 0.058 mmol) was added. The resulting solution was left to slowly evaporate at room temperature. After one week, colorless rhombic crystals suitable for X-ray diffraction analysis were obtained. The crystals were isolated and dried in open air. The yield of compound **3** was 0.018 g (31.1% based on the initial quantity of [$Tb(H_2O)_4(pfb)_3$]).

Found, %: C 41.4 H 1.6 N 2.8

For $C_{70}H_{28}F_{30}N_4O_{14}Tb_2$

Calculated, %:C 41.3 H 1.4 N 2.7

IR spectrum (ATR method; ν, cm^{-1}): 3853 w, 3801 w, 3750 w, 3710 w, 3675 w, 3628 w, 3566 w, 2900 w, 2360 m, 2163 w, 1967 w, 1793 m, 1734 m, 1673 s, 1651 s, 1594 s, 1545 m, 1522 m, 1489 s, 1449 m, 1416 s, 1393 s, 1377 s, 1352 m, 1292 m, 1223 m, 1146 m, 1106 s, 1051 m, 991 s, 940 m, 929 m, 881 w, 866 m, 842 s, 831 m, 762 m, 741 s, 727 s, 702 m, 669 m, 639 m, 619 w, 595 m, 573 w.

II. Supplementary PXRD data

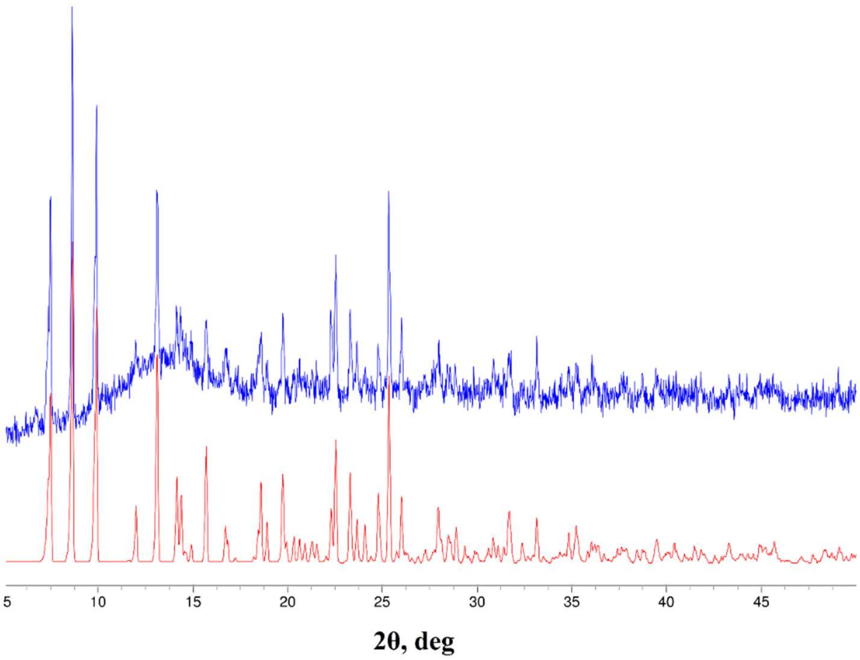

Figure S1. Theoretical (red line) and experimental (blue line) powder patterns of the compound **1**.

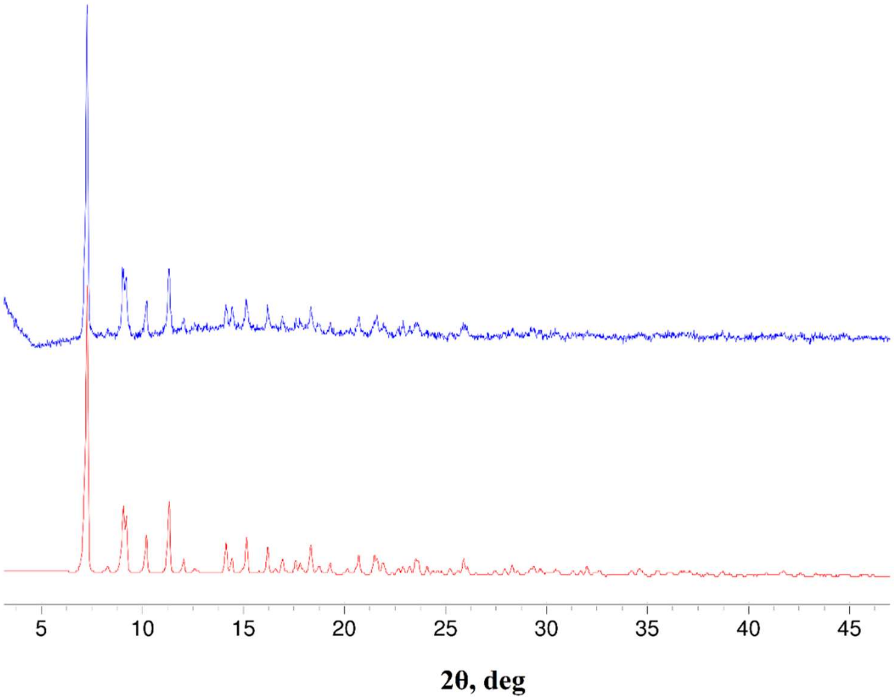

Figure S2. Theoretical (red line) and experimental (blue line) powder patterns of the compound **2**.

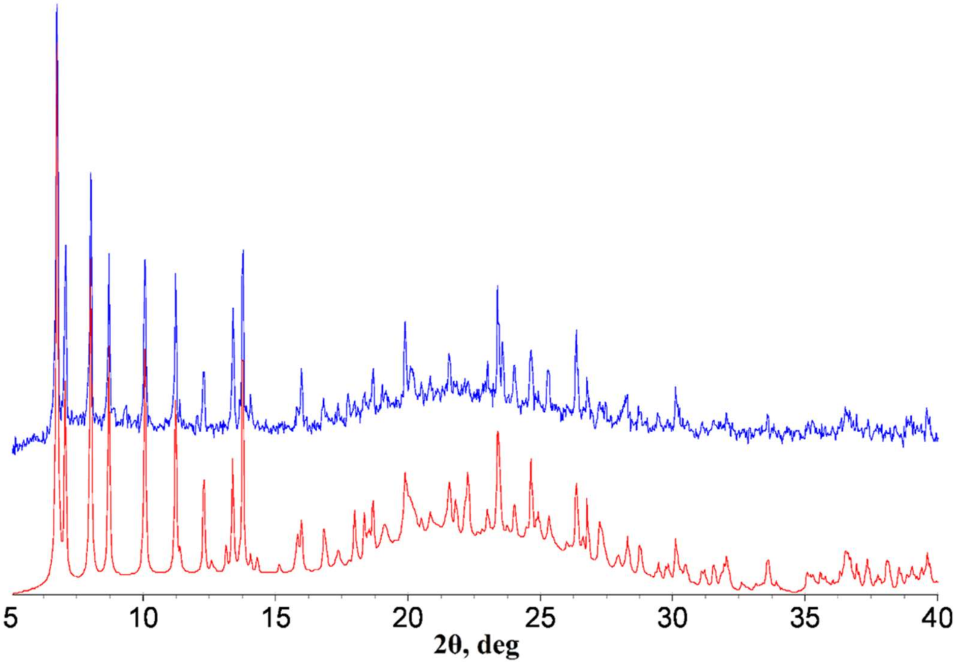

Figure S3. Theoretical (red line) and experimental (blue line) powder patterns of the compound **3**.

III. Supplementary structural data

Structural features of compound 3

Comparison of complex **3** with the previously described pentafluorobenzoate compound $[Eu_2(H_2O)_2(phen)_2(pfb)_6]$[S3] reveals that the replacement of a coordinated water molecule with a larger ethanol molecule in the case of complex **3** leads to a significant transformation of the molecule's geometry. In complex **3**, a transition from bridging coordination of pfb anions to chelating-bridging coordination occurs, resulting in a reduction of the Ln…Ln distance by 0.42 Å. The distances between the centroids of the pentafluorophenyl substituent and the coordinated molecules of 1,10-phenanthroline in the case of complex **3** are 3.74 Å, indicating a substantial enhancement of intramolecular π···π interactions compared to the known complex $[Eu_2(H_2O)_2(phen)_2(pfb)_6]$, where similar distances between centroids significantly exceed 3.8 Å.

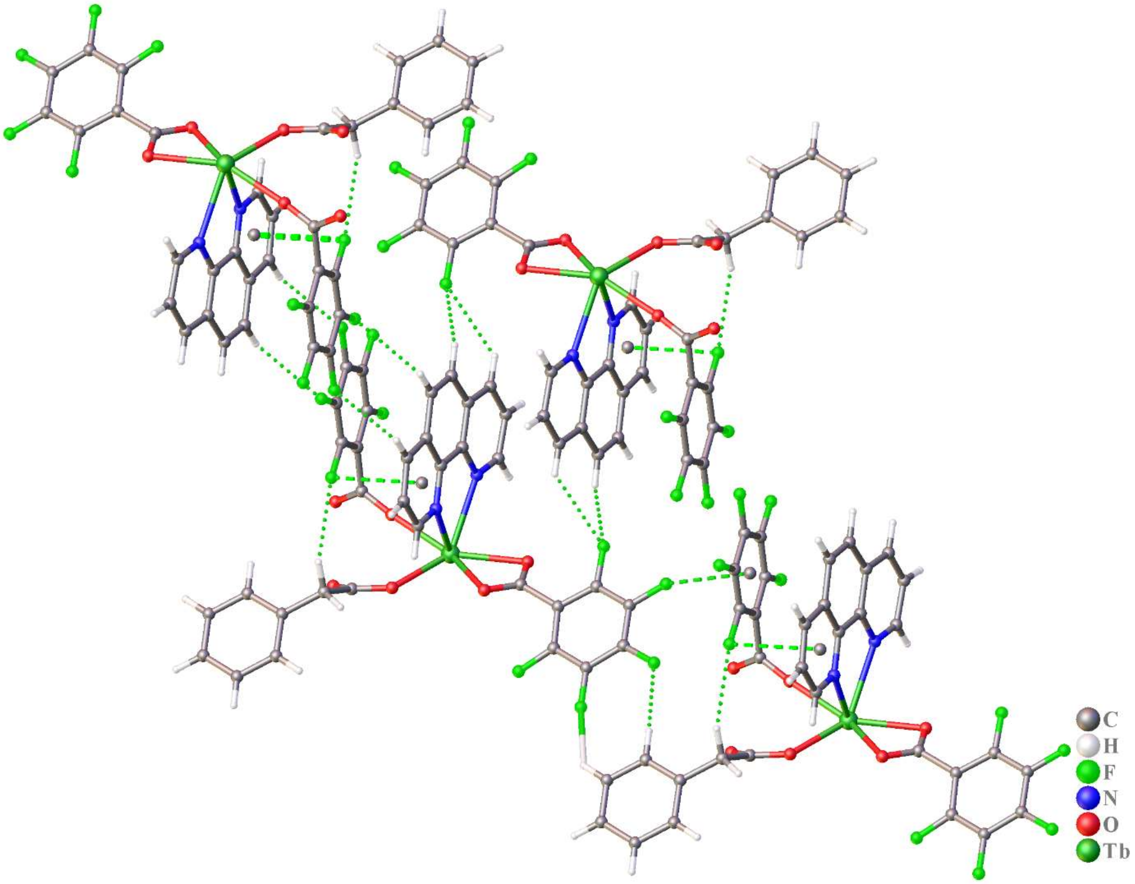

Figure S4. Fragment of complex **1** crystal packing. Intramolecular C-F···π and C-H···F interactions are represented by dashed lines. To prevent the overlap of projections, only half of the molecules from complex **1** are depicted.

Table S1. Main bond lengths and interatomic distances in the structures of complexes **1-3**

Bond	Length, Å		
	1	**2**	**3**
Tb-O(RCOO)	2.299(4)-2.466(3)	2.324(5)-2.547(5)	2.330(3)-2.560(3)
Tb-O (EtOH)	-	-	2.381(3)
Tb-N (phen)	2.544(4), 2.588(3)	2.551(6), 2.573(6)	2.553(4), 2.645(3)
Tb…Tb	4.166(1)	3.929(1)	4.045(1)

Table S2. π···π interactions in the crystal packing of complexes **1-3**.

Interaction	Cg···Cg, Å	Symmetry code	Cg···Perp, Å	α, deg
Complex **1**				
phen···pfb	3.506(3)	1-x,-y,1-z	3.314(2)	1.2(2)
pfb···PhAc	3.673(3)	2-x,1-y,2-z	3.537(2)	0.0(2)
pfb···PhAc	3.756(3)	2-x,1-y,1-z	3.427(2)	6.7(2)
phen···phen	3.634(3)	1-x,-y,1-z	3.322(2)	0.0(2)
Complex **2**				
phen···phen	3.498(5)	1-x,2-y,1-z	3.279 (3)	0.0(4)
Complex **3**				
phen···phen	3.742(3)		3.526 (2)	7.3(2)

Note. Cg — centroid of aromatic rings, Perp — perpendicular to the plane of the ring, α — angle between the planes of aromatic fragments.

Table S3. C-F···π interactions in the crystal packing of complexes **1** and **3**.

Interactions	F···Cg, Å	Symmetry code	F···Perp, Å	C-O···Cg,^{O}
Complex **1**				
C(6)–F(6)···Cg(phen)	3.133(4)	1+x,y,1+z	3.030	148.8(3)
C(14)–F(14)···Cg(pfb)	3.251(3)		3.243	95.7(2)
Complex **3**				
C(3)–F(3)···Cg(phen)	3.436(3)		3.176	79.8(3)
C(13)–F(13)···Cg(pfb)	3.551(4)	3/2-x,1/2+y,3/2-z	3.500	95.5(2)

Note. Cg — centroid of aromatic rings, Perp — perpendicular to the plane of the ring, α — angle between the planes of aromatic fragments.

Table S4. Hydrogen bonds in the crystal packing of complexes **1-3**.

Interaction	Distance, Å				D – H···A, °
	D–H	Symmetry code	H···A	D···A	
Complex **1**					
C(19)–H(19)···F(4)	0.95	-1+x,y,-1+z	2.49	3.213(6)	133
C(23)–H(23)···O(5)	0.95		2.59	3.068(6)	112
C(28)–H(28)···F(7)	0.95	1-x,-y,1-z	2.54	3.338(6)	141
C(32)–H(32)···O(6)	0.95	1-x,1-y,1-z	2.47	3.025(6)	117
Complex **2**					
C(10)–H(10A)···O(5)	0.99	-1+x,y,-1+z	2.57	3.411(11)	143
C(25)–H(25)···O(1)	0.95		2.50	3.037(11)	116
C(27)–H(27)···O(4)	0.95	1-x,-y,1-z	2.36	3.245(10)	155
C(32)–H(32)···O(6)	0.95	1-x,1-y,1-z	2.54	3.383(10)	148
C(34)–H(34)···O(2)	0.95	1-x,1-y,1-z	2.40	3.069(10)	127
Complex **3**					
O(7)–H(7)···O(5)	0.88		2.54	2.832(4)	100
C(22)–H(22)···O(4)	0.95	x,1/2-y,1/2+z	2.41	2.915(6)	113
C(26)–H(26)···F(12)	0.95		2.55	3.044(6)	113
C(31)–H(31)···O(3)	0.95	1-x,1-y,1-z	2.34	2.982(6)	125

Table S5. Contribution of noncovalent interactions to the Hirshfeld surface of complexes **1-3**.

Interaction	Complex		
	1	**2**	**3**
C···C	7,6%	4,1%	2,1%
C···F	6,7%	-	12,1%
H···F	31,7%	-	41,2%
O···H	6,4%	10,7%	4,8%
C···H	11,6%	31,0%	8,0%

IV. Supplementary photoluminescent data

It is known that in the presence of a single type of emitting center - ion, an asymmetric ligand field can mix with states of the ion with opposite parity in the 4f^n shell, thereby partially lifting the prohibition of electric dipole transitions, leading to an increase in the rate of radiative relaxation[S4]. To assess the symmetry of the coordination environment of Tb^{3+} ions in the studied compounds, the branching coefficient β was calculated as the ratio of the integral intensities of the electric dipole transition ($^5D_4 \rightarrow {}^7F_6$, $\Delta J = 2$) and the magnetic dipole transition ($^5D_4 \rightarrow {}^7F_5$, $\Delta J = 1$). It was found that all studied complexes have a sufficiently high value of β (0.25 for complex **1**; 0.25 for complex **2**; 0.34 for complex **3**). This indicates a low ligand field symmetry. The lowest degree of symmetry is observed for complex **3** (β=0.34), indicating the highest probability of radiative relaxation for this complex. Therefore, for complex **3**, we expect the highest quantum yield[s5].

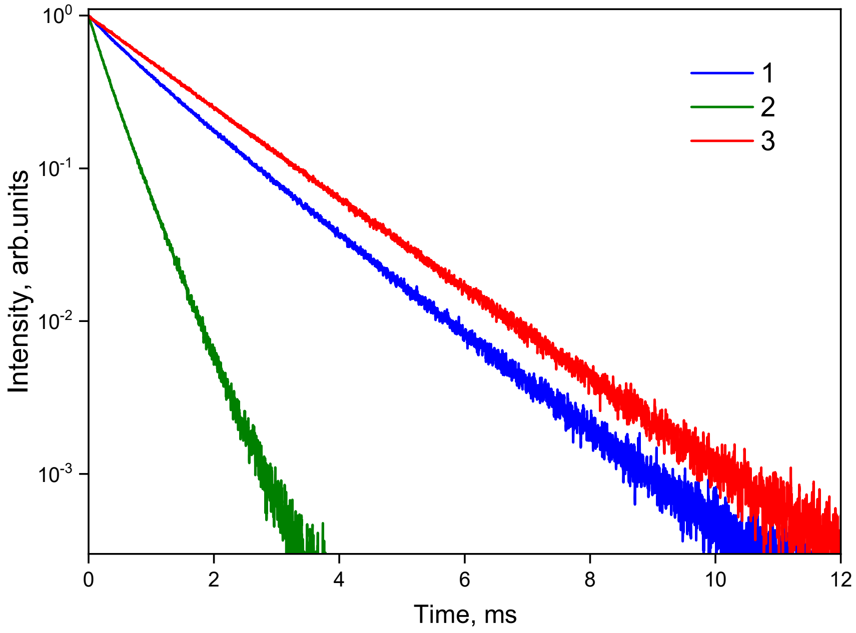

Figure S5. PL decays for **1**, **2**, **3** compounds in crystalline powder at 300 K upon pulsed excitation at 330 nm registered at 547 nm.

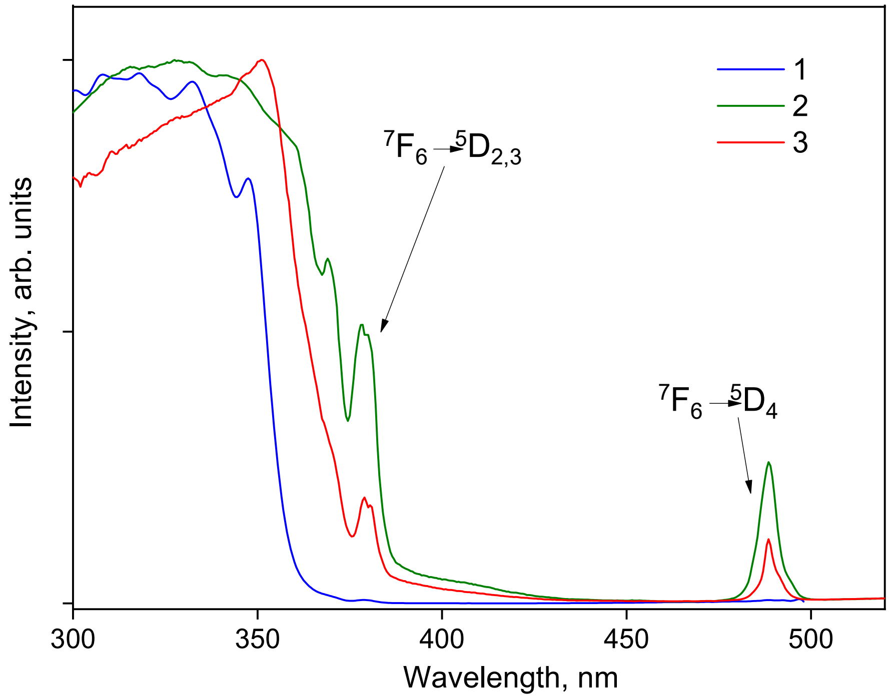

Figure S6. Optical excitation spectra of **1**, **2** and **3** crystalline powder compounds recorded at room temperature with registration at 547 nm.

V. References

S1. S. V. Larionov, L. A. Glinskaya, T. G. Leonova, R. F. Klevtsova, E. M. Uskov, V. E. Platonov, V. M. Karpov and V. P. Fadeeva, *Russ. J. Coord.Chem.*, 2009, **35**, 798.

S2. N. V. Y. Scarlett and I. C. Madsen, *Powder Diffr.*, 2006, **21**, 278.

S3. L.-J. Han, Y.-J. Kong, N. Sheng and X.-L. Jiang, *J. Fluorine Chem.*, 2014, **166**, 122.

S4. S. Katagiri, Y. Tsukahara, Y. Hasegawa and Y. Wada, *Bull. Chem. Soc. Jpn.*, 2007, **80**, 1492.

S5. D. M. Roitershtein, L. N. Puntus, A. A. Vinogradov, K. A. Lyssenko, M. E. Minyaev, M. D. Dobrokhodov, I. V. Taidakov, E. A. Varaksina, A. V. Churakov and I. E. Nifant'ev, *Inorg. Chem.* 2018, **57**, 10199.